Vol. 5 No. 1, June, 2025

FUAM Journal of Pure and Applied Science

Available online at
www.fuamjpas.org.ng

An official Publication of
College of Science
Joseph Sarwuan Tarka University,
Makurdi.

FUAM Journal of Pure and Applied Science
© College of Science, Joseph Sarwuan Tarka University, Makurdi
https://fuamjpas.org.ng/
Vol.5 No. 1 June, 2025

Anti-Plasmodial Activity of Iron Oxide Nanoparticles Derived from *Moringa Oleifera* Stem Bark and Root Extracts

O.M[1*]. Fayomi, O.O[2]. Olajide and S.A[2]. Emmanuel
[1]Department of Chemistry, Faculty of Physical Science, Joseph Sarwuan Tarka University, Makurdi. Nigeria.
[2]Chemistry Advanced Research Centre, Sheda Science and Technology Complex (SHESTCO), Abuja, Nigeria.
[*]Correspondence E-email: omotolafayomi@gmail.com

Received: 03/07/2024 **Accepted**: 07/08/2024 **Published online**: 09/08/2024

Abstract
Malaria, caused by Plasmodium parasites, requires a comprehensive treatment strategy, involving the use of phytochemicals, marine organisms, synthetic substances, and nanomaterials. Iron oxide nanoparticles (IONPs) are increasingly attracting attention in medical research because of their biocompatibility, facile degradation, and minimal toxicity. This work presents the results of biosynthesis of IONPs from the extracts of *Moringa oleifera* stem bark and roots, regions that have been relatively unexplored despite their recognized medicinal properties. Characterization of the IONPs was conducted through SEM, XRD, FTIR, and UV-visible spectroscopy. The UV-Vis spectroscopic analysis exhibited distinctive absorption peaks, with IONPsSTEM peaking at 300 nm and IONPsROOT ranging between 300–400 nm. The FTIR spectra illustrated characteristic bands assigned to Fe-O, C=O, and O-H. Examination of SEM images unveiled agglomerates of flattened spherical and spindle-shaped hematite, corroborated by EDX and XRD data. The antiplasmodial efficacy of both variants of IONPs demonstrated moderate effectiveness against Plasmodium parasites, surpassing the crude extracts of the stem and root extracts, albeit falling short of the efficacy of Artemether.
Keywords: Anti-Plasmodial Activity, Iron Nanoparticles, Stem Bark, Root Extracts, Moringa Oleifera

Introduction

Malaria has consistently been a global burden. A recent World Health Organization (WHO) report estimated 249 million global population spread across 85 malaria-endemic countries and territories were affected, a notable 5 million cases surge from the preceding year. The global malaria-related mortality which had been steadily declining before 2022 had a slight increase to 608,000 deaths in 2022. This proportion of cases attributable to *Plasmodium vivax* also affects pregnant women whose infection could result in neonates with low birth weight (1).

Malaria, caused by Plasmodium parasites, unfolds through a complex lifecycle involving transmission and fertilization within hosts (2). Notably, *Plasmodium berghei* in rodent hosts mimics the human malaria lifecycle, infiltrating red blood cells (RBC) similarly. Severe *P. berghei* infection in rodents reflects clinical manifestations observed in humans, including vital-organ dysfunction and anaemia (3). Additionally, *P. vivax* and *P. ovale* infections introduce dormant hypnozoites, potentially causing relapses. While uncomplicated falciparum malaria has a low mortality rate, severe cases can lead to organ dysfunction or increased parasitic burden. Severe malaria manifests with diverse clinical symptoms, including coma and jaundice. Septicemia, often complicating severe malaria, underscores its nuanced nature, particularly in vulnerable populations (4).

Mitigating these Plasmodium parasites requires a multifaceted approach, including the exploration of various compound classes derived from plants (5), marine organisms (6), microbes (7), synthetics (8), and nanomaterials (9). Plant-derived compounds are rich sources of active biomolecules, such as alkaloids, terpenoids, flavonoids, polyphenols, essential oils, and extracts from medicinal plants like *Cissampelos pareira* (10), *Commiphora spp* (11) and *Neorautanenia mitis* (12). These compounds exhibit diverse pharmacological activities, along with their anti-malarial potential. Similarly, marine-derived compounds, including marine natural products (13), algae extracts (14), sponge-derived compounds (15), and coral-derived compounds (16), hold promising antimalarial properties, utilizing their marine biodiversity in drug discovery. Microbial-derived compounds, such as antibiotics (17), antifungal agents (18), and bacterial (19) and fungal metabolites (20) are repurposed by leveraging the vast biochemical diversity of microorganisms in inhibiting malaria. Synthetic compounds, including analogs of natural products (21), small molecules (16), peptides (22), and polymers (23), provide synthetic versatility and

optimization opportunities for antimalarial drug development.

Among these categories, nanomaterials hold particular significance due to their unique physicochemical properties and potential for targeted drug delivery and enhanced therapeutic efficacy (24). Metal nanoparticles (25), metal oxide nanoparticles (26), carbon-based nanomaterials (27), and lipid-based nanoparticles (28) exhibit distinct advantages in terms of stability, biocompatibility, and tunable surface properties, which can be tailored to optimize drug loading, release kinetics, and biodistribution. The application of nanomaterials in malaria treatment poses several advantages over conventional drug formulations, including improved pharmacokinetics, reduced drug resistance, and enhanced cellular uptake, leading to higher intracellular drug concentrations at the site of action (29). Nanomaterial-based drug delivery systems facilitate the co-delivery of multiple therapeutic agents, allowing for synergistic effects and combinatorial therapies to overcome drug resistance and enhance treatment outcomes (30).

Iron oxide nanoparticles (IONPs), as metal nanoparticles have increasing research interests in medicine because of their biocompatibility, biodegradability, and low toxicity (31,32). Their synthesis through chemical methods, with the co-precipitation approach stand out for its efficiency and high yield (33). IONPs serve as indispensable tools in magnetic resonance imaging (MRI) (34), targeted drug delivery systems (35), cancer immunotherapy (36), and as hyperthermia mediators (37), proffering diverse solutions to complex medical challenges. Iron oxide shows antimicrobial potential and generate reactive oxygen species (ROS) which induce oxidative stress, damage or death on parasitic cell (38). However, ensuring the biocompatibility and safety of iron nanoparticles remains paramount, necessitating a thorough understanding of their properties, including size, surface coating molecules, and functional groups (39).

IONPs are synthesized by chemical methods such as co-precipitation (40), thermal decomposition (41), hydrothermal (42), solvothermal (43), microemulsion (44), sol-gel (45), polyol (46), ultrasonic-assisted (47), and electrochemical techniques (48). These methods, though, give good IONPs yields, they are challenged with issues like particle size control, complex setups, and the use of hazardous reagents. The green synthetic approaches however, offer better eco-friendly, low toxic and sustainable solutions. These methods leverage on renewable resources such as plants (49) and microorganisms (50), making them inherently safer and more sustainable. The plant extracts reduces and stabilizes the iron ion using their metabolites to give IONPs during the synthesis (51).

Leaves, seeds, and fruits of plants are rich in biomolecules and widely reported for their role in the synthesis of IONPs. Leaves, in particular, are popular due to their abundance, affordability, and availability, providing essential metabolites for metal reduction and nanoparticle capping. Extracts from various plant parts such as *Prunus persica* leaves (52), *Laurus nobilis* leaves (53), *Moringa oleifera* leaves (54), and *Moringa oleifera* seeds (55) have been successfully used to synthesize IONPs, acting as both capping and reducing agents. Although there are fewer studies utilizing extracts from stem bark, and roots for IONPs synthesis, their potential remains significant (56) (57). Despite the bioactivities of *Moringa oleifera* stem bark and roots (58), their use in IONPs synthesis has not been explored. This study is aimed at synthesizing IONPs from *Moringa oleifera* stem bark and root extracts and investigation of their anti-plasmodial activities in an *in vivo* model, addressing the knowledge gap.

Materials and Method

Materials

Iron (III) chloride hexahydrate ($FeCl_3{\cdot}6H_2O$), sodium hydroxide (NaOH), ethanol 99.9% of analytical grade (Molychem products) were obtained from a commercial dealer and used without any additional reagents. All the glassware was washed with deionized water and oven dried. The standard antimalarial drug Artemether was obtained commercially. *Moringa oleifera* stem barks and root were freshly collected from the Medicinal Garden at Sheda Science and Technology Complex (SHESTCO), Abuja. The plants were identified by a botanist, Mr Akeem Lateef and the specimen voucher number (NIPRD/H/7405) was deposited at National Institute of Pharmaceutical Research and Development, NIPRD, Idu, Nigeria. The deionized water was used for all the homogenization process.

Preparation of Moringa oleifera Stem Bark and Root Extract

To prepare the extract of *Moringa oleifera* stem barks, the barks were washed with deionized water to remove impurities, air dried and pulverized. The fine powdered *Moringa oleifera* stem bark of 6g was added into 200 mL deionized water which was heated at 100°C for 20 to 30 minutes. The obtained extract was filtered using filter paper (Whatman no. 1) and stored at 4°C for further use (59).

Similar method was used to obtain *Moringa oleifera* root extract.

Synthesis of IONPs of Moringa Oleifera Stem Bark and Root Extract

The 50 mL extract of *Moringa oleifera* stem barks was added dropwise with 50 mL of 0.001M (3.244g) $FeCl_3{\cdot}6H_2O$ solution and continuously stirred to add 1 M NaOH solution. Brown precipitates appeared which was stirred for 1 hour 30 minutes at 70°C on a magnetic hotplate. The colour change confirmed the formation of IONPs which was centrifuged at 3000 rpm in 20 minutes, washed with ethanol and oven dried at 90°C for 3 hours. The reddish brown powder obtained was calcined at temperature at 450 °C for 2 hours (60).

Similar procedure involving the extract of *Moringa oleifera* root was used to obtain other IONPs.

Characterization of Iron Oxide Nanoparticles of M. oleifera Stem and Root Extract

The UV-VIS characterization involved JENWAY 6405 UV-Vis spectrophotometer to confirm and characterize the synthesis of IONPs. The UV–Vis absorption spectrum was validated through a wavelength scan spanning from 200 to 800 nm. Having synthesized IONPs through the biogenic method, the UV-Vis spectra of the solution was taken at different wavelengths.

FTIR analysis provides spectroscopic information about bond details of compounds. For these green synthesized IONPs, FTIR spectra were recorded on an Agilent 630 Cary FTIR Spectrometer. This model of spectrometer has two modules - an ATR module for liquids and solids, and a 'Dial Path' module for absorbance spectra of liquids, films and gels. For this analysis, the IONPs were prepared on KBr discs using a 4% (w/w) solid/KBr mixture. The FTIR spectra were acquired in the range of 400–4,000 cm^{-1}. The vibrational mode along with the bond details of compounds was studied. Likewise, the biomolecules present in plant extract at 1 mm thick re-crystallized KBr disc.

The X-ray Diffractometer (XRD) Thermo scientific model: ARL 'XTRA X-ray and serial number 197492086 analyzed the materials. XRD characterization of thin film of each sample was done in Umaru Musa Yar'adua University, Katsina State, Nigeria. As a non-destructive analytical technique for characterizing crystalline materials, information regarding the structures, phases, texture, crystal lattice parameters, chemical composition and other structural parameters such as average grain size, crystallinity, crystal defects and strain could be obtained.

The materials also were analyzed by EDX Scanning Electron Microscope (SEM) model: PRO:X: 800-07334 Phenom World and serial number MVE01570775. This analytical technique gives information regarding the structures, surface morphology of the materials. It was as well performed pore and fibre metric analysis together with particles sizes on the IONPs.

$$\% \text{ Parasite Growth} = \frac{Number\ of\ Parasitized\ Cells\ x\ 100}{Number\ of\ Red\ Blood\ Cells\ (RBC)} \quad (1)$$

$$\% \text{ Inhibition} = \frac{\%\ Parasitaemia_{control} - \%\ Parasitaemia_{test\ group}\ x\ 100}{\%\ Parasitaemia_{control}} \quad (2)$$

Statistical Analysis

The collected data from the *in vivo* exercise were analyzed using OriginPro Software® 2017 with the results of study expressed as a mean ± standard error of the mean (M±SE). One-way analysis of variance (ANOVA) was used to compare between groups followed by Tukey and Levene post-hoc. Differences of $p < 0.05$ were considered significant.

Experimental Animals

For experimental purpose, Winstar rats obtained from the College of Veterinary Medicine, Joseph Sarwuan Tarka University, Makurdi were housed in a 15x30cm cage with metal tops. The cage was regularly maintained with constant change of the wood shavings (saw dust) serving as bedding materials. The experimental rats grouped into six were acclimatized for 2 weeks. Each of these groups made up of 2 rats was treated separately with the stem bark and root extracts of *Moringa Oleifera* along with their corresponding IONPs as the test groups while the remaining groups had positive and negative controls. The positive control was treated with Artemether tablet. The negative control, however, was neither treated nor induced.

Suppression of Plasmodium Parasites by IONPs

The IONPs suppression of the Plasmodium parasites was deduced along with the extracts of *Moringa Oleifera* stem bark and root (the capping agents), then the positive and negative controls in agreement with some reports (61). About 2mL of fresh blood was collected from the two weeks acclimatized rats (115 – 120 g) and was mixed with 0.6mL of normal saline. The 0.5 mL parasitaemia (1×10^7 *Plasmodium berghei*) in blood saline suspension was administered intraperitoneally as infection on the rats and were left for 24 hours to allow the Plasmodium parasites spread.

Afterwards, treatments by each extract of the stem and roots of *Moringa oleifera* along with their corresponding IONPs and positive control (Artemether) were carried out at 50 mg/kg body weight. After 48 hours, the blood samples from pricked tail of the experimental rats were taken unto a clean glass slide, smeared to make a thin blood film, air-dried and mixed with methanol for 1 hour. Then staining with giesma stain for 10 minutes and rinsed. When dried, each specimen was viewed under the microscope of x100 objective lens (62) (63). The percentage parasite growth and percentage inhibition on the red blood cells (RBC) were determined using the given equations (1) and (2):

Results and Discussion

Biosynthesis of IONPs

The biosynthesis of iron oxide nanoparticles (IONPs) was achieved by reducing and stabilizing iron salts in an aqueous solution using *Moringa oleifera* extracts. The synthesis involved reacting ferric chloride with extracts from the stem and root of *Moringa oleifera*, which resulted in a colour change of the reaction mixture to reddish-brown, indicating the formation of IONPs.

UV–Vis Spectra of Biosynthesized IONPs

Investigating the optical properties of the green synthesized iron oxide nanoparticles (IONPs), UV-Vis absorption spectra were recorded, as shown in Figure 1.

The UV-Vis spectroscopy displayed an absorption peak at 300 nm in the UV region, indicating the formation of IONPs using Moringa oleifera stem bark extracts (IONPsSTEM) (64). This peak, due to the quantum confinement effect, sets these nanoparticles apart from bulk iron oxide materials (65). Importantly, the absence of additional peaks associated with impurities and defects indicates the high purity and quality of the crystalline biosynthesized IONPs from stem extracts. Similarly on the spectra (Figure 1), the UV-Vis absorption confirmed the formation of IONPs from root extracts (IONPsROOT), showing an absorption peak in the range 300 – 400 nm with no extra peaks, which further validates the IONPs were qualitatively pure (66).

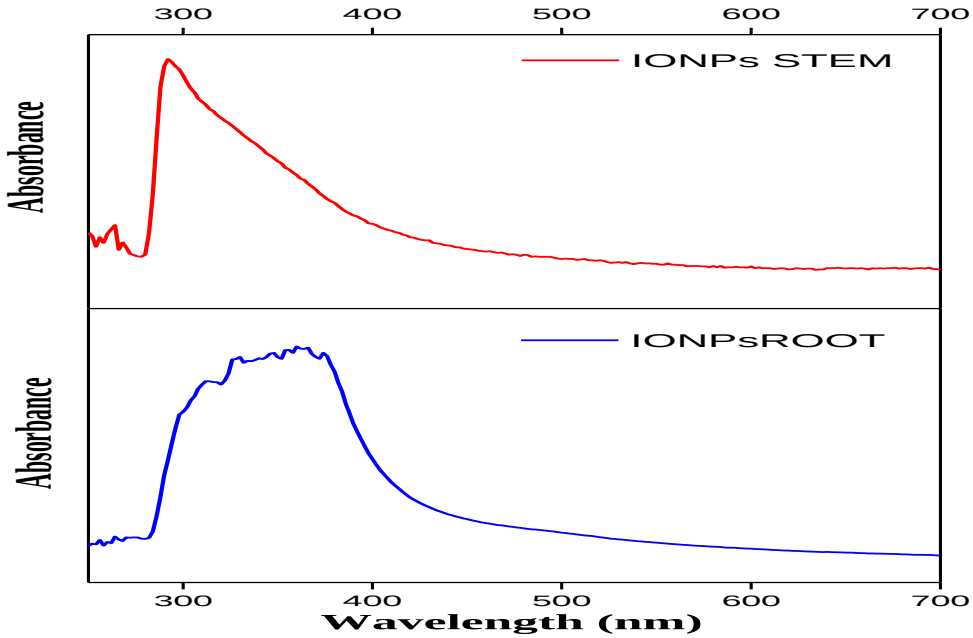

Figure 1: UV-Visible Spectra of IONPsSTEM and IONPsROOT

FTIR Analysis of IONPs

The Fourier Transform Infrared (FTIR) spectroscopic analysis of biosynthesized iron oxide nanoparticles (IONPs) from *Moringa oleifera* stem and root extracts gave absorption bands indicative of specific functional groups. For IONPsSTEM, as shown in Figure 2, the absorption bands at 797 cm^{-1}, 1036 cm^{-1}, and 1394 cm^{-1} were attributed to the stretching vibrations of Fe−O bonds, C−O stretching, and C−H bond stretching, respectively (67). The band at 1610 cm^{-1} was associated with the C=O stretching of amide groups, while the bands at 1893 cm^{-1}, 1990 cm^{-1}, and 2109 cm^{-1} were linked to various functional groups present in the stem extract. Additionally, the band at 2892 cm^{-1} indicated C−H bond stretching, and the broad band at 3220 cm^{-1} was due to hydroxyl (O-H) stretching. Similarly, the root-derived IONPs in Figure 2b, showed an absorption band at 685 cm^{-1} for Fe−O bond stretching, 1625 cm^{-1} for C=O stretching of amide groups, and bands at 1871 cm^{-1}, 2117 cm^{-1}, and 2340 cm^{-1} for various organic functional groups (68). The bands at 2802 cm^{-1} and 2884 cm^{-1} were associated with C−H bond stretching, and the band at 3250 cm^{-1} was due to O−H stretching. The deduction from the findings suggest the reducing and capping ability of the biomolecules in the *Moringa oleifera* extracts on the iron salts (69).

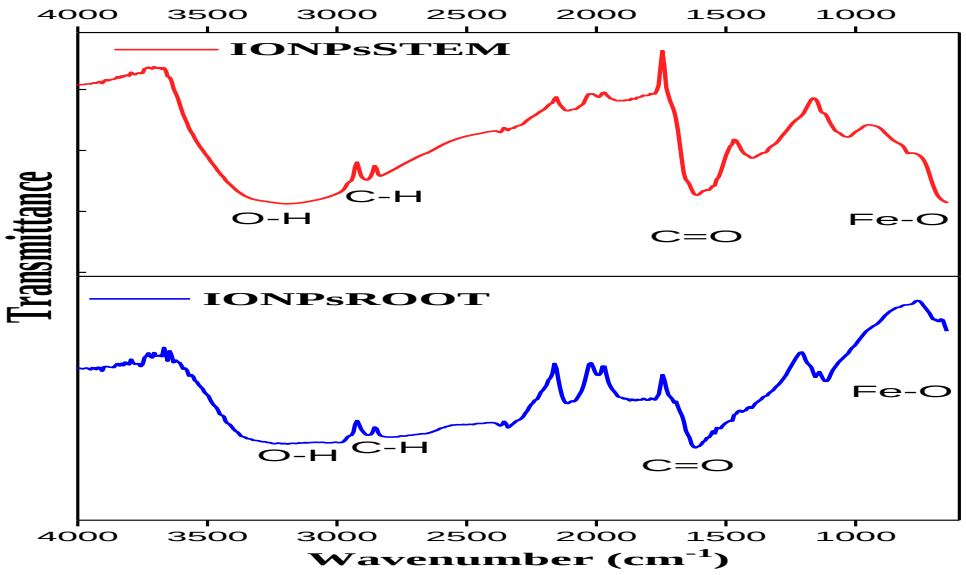

Figure 2: FTIR Spectra of IONPsSTEM and IONPsROOT

SEM Analytical Technique

The surface morphology and size of the synthesized IONPs derived from *Moringa Oleifera* stem bark and root extract were analyzed by SEM. The SEM images in Figures 3a, b, c and d for respective 5µm and 1 µm magnifications. The images revealed an interaction between iron and the biomolecules of the plant extracts resulting in spherically flattened hematite (70) and spindle hematite shapes (71) respectively. The SEM images are agglomerated with the chunk of particles in micro range, i.e. the presence of bioactive substances originating from plants capping the metal element.(72).

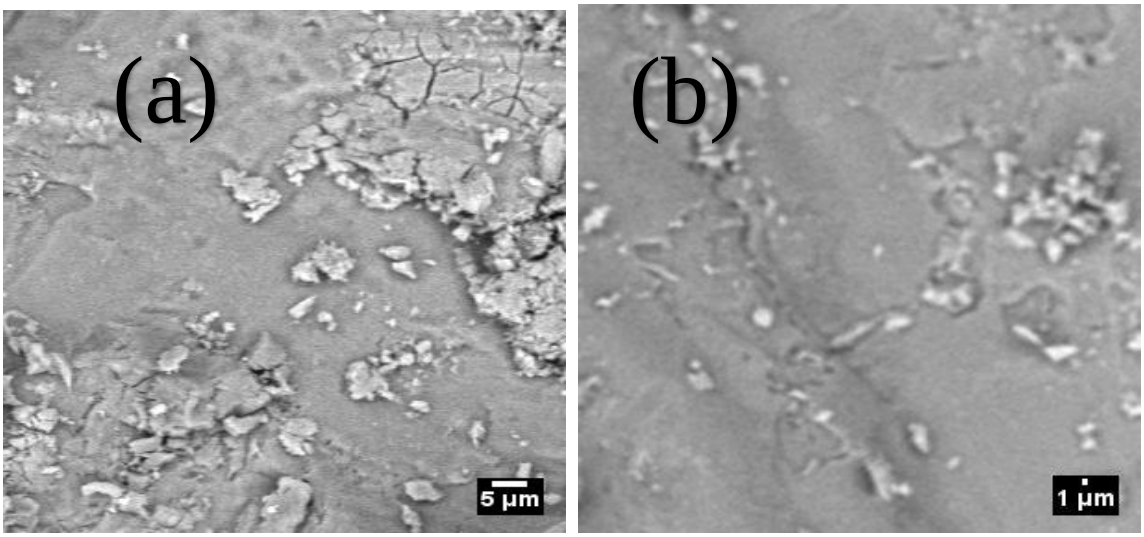

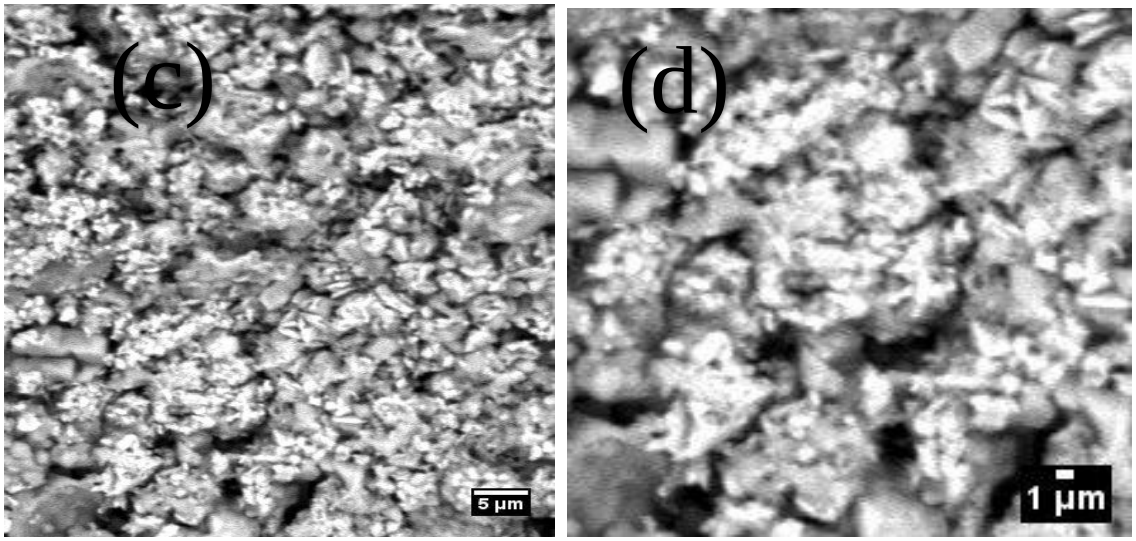

Figure 3: SEM Images of (a) IONPsSTEM at 5µm (b). IONPsSTEM at 1 µm (c) IONPsROOT at 5µm (d) IONPsROOT at1 µm

EDX Analysis of IONPs

The elemental composition analysis of the iron oxide nanoparticles (IONPs) confirmed the presence of iron as shown in figures 4a and b, affirming the purity of the biosynthesized IONPs. In Tables 1 and 2, the relative percentage of iron in the nanoparticles derived from stem bark and root were found to be 14.69% and 61.82%, respectively. These values, clearly highlighted in Figures 4a and b, closely align with the theoretically expected stoichiometric mass percentages, indicating the successful synthesis and high purity of the IONPs (73).

Table 1: EDX Weight Ratio of Electrospun IONPsSTEM

Element Number	Element Symbol	Element Name	Atomic Conc.	Weight Conc.
26	Fe	Iron	8.10	14.69
17	Cl	Chlorine	39.24	45.14
11	Na	Sodium	48.92	36.50

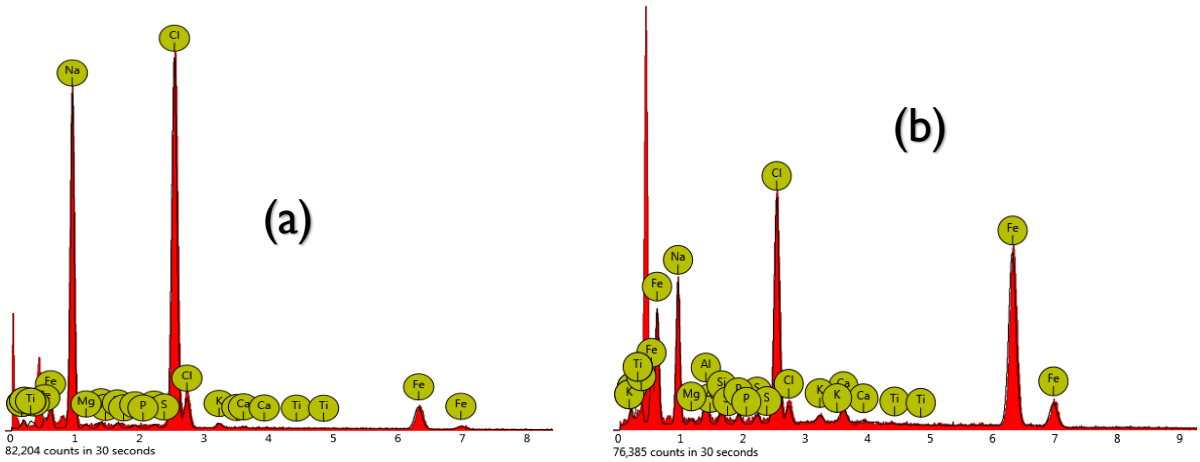

Figure 4: EDX of (a) IONPsSTEM (b) IONPsROOT

Table 2: EDX Weight Ratio of Electrospun IONPsROOT

Element Number	Element Symbol	Element Name	Atomic Conc.	Weight Conc.
26	Fe	Iron	45.35	61.82
17	Cl	Chlorine	18.44	15.96
11	Na	Sodium	25.98	14.58

XRD Pattern of IONPs

The Powder XRD patterns of biosynthesized iron oxide nanoparticles (IONPs) derived from both the stem bark and root extracts of *Moringa oleifera* are presented in Figure 5, respectively. The diffraction peaks for the stem bark-derived IONPs can be indexed to the flattened form of hematite (Fe_2O_3) crystals, according to JCPDS card No. 00-002-0837. The observed peak positions at 2θ values of 29.14°, 32.28°, and 45.98° correspond to the crystal planes (104), (113), and (024), respectively (74). Similarly, the root-derived IONPs showed diffraction peaks consistent with the spindle form of hematite, with peak positions at 2θ values of 24.28°, 33.38°, 35.17°, 38.3°, 42.7°, 45.60°, 49.70°, 54.28°, 57.62°, 58.96°, 64.22°, and 69.94°, corresponding to the crystal planes (012), (104), (110), (006), (113), (202), (024), (116), (122), (018), (300), and (208) respectively (75).

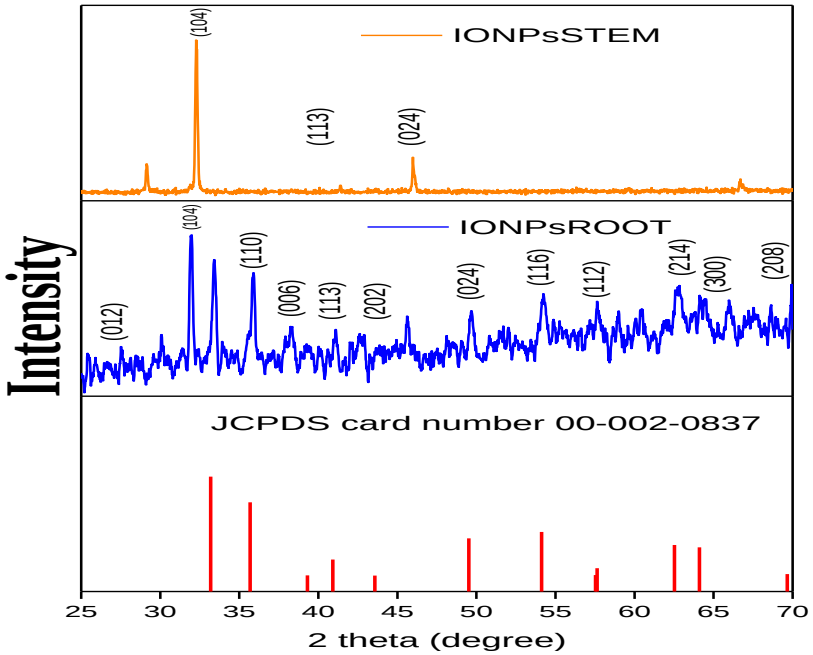

Figure 5: XRD patterns for synthesized IONPsSTEM, IONPsROOT showing different peak positions at 2θ along with the JCPDS card number 00-002-0837 indicating the miller indices of the synthesized nanoparticles.

The crystallite sizes of these IONPs were calculated using the Scherrer equation (3),

$$D = \frac{K\lambda}{\beta \cos\theta} \qquad (3)$$

where D is the crystallite size, K is the Scherrer constant (0.9), λ is the X-ray wavelength (0.1541 nm), β is the full width at half maximum (FWHM) of the diffraction peak, and θ is the peak position (76). From Table 3, the stem bark-derived IONPs, the crystallite sizes ranged from 47.86 nm to 62.23 nm, with an average size of 52.91 nm, while root-derived IONPs as shown in Table 4, ranged from 4.43 nm to 38.57 nm, with an average size of 12.96 nm. The peak broadening in the XRD patterns indicates the presence of small nanocrystals. The calculated crystallinities according to equation (4) were 13.98 and 38.86 for the stem bark and root extracts, respectively, further supporting the formation of nanocrystals (77).

$$\text{Crystallinity} = \frac{Area\ of\ crystalline\ peaks}{Area\ of\ all\ peaks\ (crystalline+amorphous)}\ x\ 100 \qquad (4)$$

Table 3: Some Crystallographic Parameters of the Synthesized IONPsSTEM based on the X-Ray Diffraction Pattern

S/N	Peak Position (2θ)	FWHW (β) (degree)	Crystallite size D (nm)	D (Average) (nm)
1	29.14	0.1533	53.55	52.91
2	32.28	0.1728	47.86	
3	45.98	0.1387	62.23	
4	66.70	0.1982	47.99	

Table 4: Some Crystallographic Parameters of the Synthesized IONPsROOT based on the X-Ray Diffraction Pattern

S/N	Peak Position (2θ)	FWHW (β) (degree)	Crystallite size D (nm)	D (Average) (nm)
1	24.28	0.6493	12.5154	12.9666
2	31.96	0.3291	25.1082	
3	33.38	0.4121	20.1274	
4	35.86	0.4919	16.9732	
5	38.30	0.7737	10.8697	
6	41.04	0.7749	10.9469	
7	42.70	1.0659	8.0026	
8	45.60	1.3843	6.2251	
9	49.70	0.5422	16.1461	
10	54.28	0.7660	11.6543	
11	57.62	1.5336	5.9118	
12	58.96	1.1475	7.9528	
13	60.48	2.0740	4.4336	
14	62.78	1.9800	4.7002	
15	64.22	1.2800	7.3274	
16	69.94	0.2514	38.5703	

Antiplasmodial Activity of Biosynthesized IONPs of Moringa Oleifera Stem and Root Extract

The anti-plasmodial activity of iron oxide nanoparticles (IONPs) derived from *Moringa oleifera* stem and root extracts as shown in Figures 6 and 7 was evaluated against Plasmodium parasites, showing moderate activity compared to the positive control Artemether (78). *In vivo* tests on experimental rats revealed in Figure 7 that IONPs from the stem extract inhibited parasitaemia by 48.58±1.77%, while the root-derived IONPs exhibited a parasitaemia inhibition of 52.24±6.40% (79). These results as shown in Table 5 were compared to the *M. oleifera* stem and root extracts alone, which showed lower inhibition rates. The study demonstrated the potential of IONPs synthesized from *M. oleifera* extracts as effective anti-malarial agents, with the positive control Artemether exhibiting the highest inhibition rate at 70.45±0.00% (80).

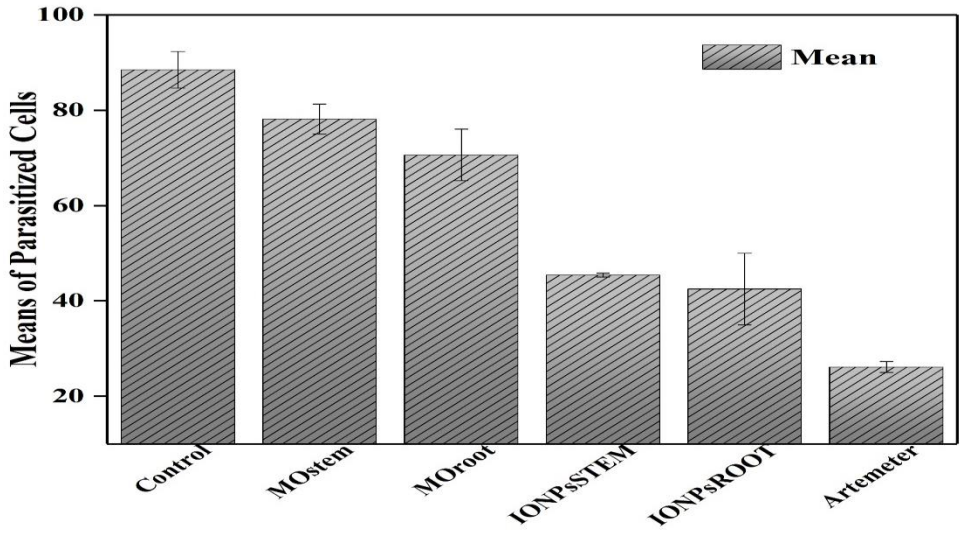

Figure 6: Number of parasitized cells of the Negative Control and Test Groups of Winstar Rats. All Values are presented as mean±SEM p<0.05 was considered significant for comparison.

Table 5: Antiplasmodial Activity of IONPs and their Respective *Moringa Oleifera* Stem amd Root Extract along with the Positive Control (Artemether) against *Plasmodium berghei*

Samples	Negative Control	*M. Oleifera Stem Extract*	*M. Oleifera Root Extract*	IONPsSTEM	IONPsROOT	Artemether
% Inhibition on the Parasites	0	11.36±7.39	20.30±2.36	48.58±1.77	52.24±6.40	70.45±0.00

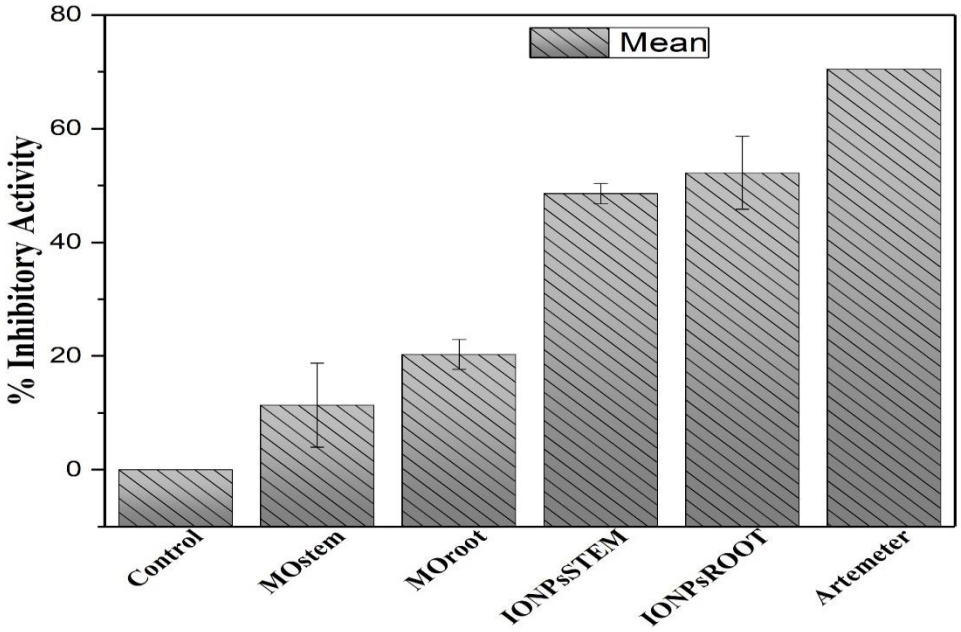

Figure 7: *In vivo* Anti-plasmodial Activity in percentage of IONPsSTEM, IONPsROOT, their *Moringa Oleifera* Stem and Root Extracts, Artemether (Positive Control) and Negative Controlled Rats. Values are presented as mean±SEM p<0.05 was considered significant for comparison.

Iron oxide nanoparticles (IONPs) synthesized from the stem and root of *Moringa oleifera* demonstrate strong anti-plasmodial effects, particularly when paired with phytochemicals that boost immune response. Upon entry into infected red blood cells, these IONPs discharge iron ions, prompting oxidative stress crucial for impairing the parasite's nucleus, effectively suppressing Plasmodium proliferation and surpassing the efficacy of these plant extracts alone (79). The significance of iron in combatting pathogens is necessitated by the performance of IONPs derived from diverse plant sources such as *Nephrolepis exaltata*, *Camellia sinensis*, *Matricaria chamomilla L.*, *Artemisia herba-alba Asso*, and *Punica granatum L.* peel, which are of notable antimicrobial properties against a range of pathogens, including both gram-positive and gram-negative bacteria, underscoring the importance of iron in inhibiting pathogenic activity (81).

Conclusion

The eco-friendly synthesis of IONPs derived from *Moringa oleifera* stem and root extracts was successfully carried out and characterized by UV-VIS, FTIR, SEM, EDX, and XRD. These nanoparticles, with average grain sizes of about 52.9 nm and 12.9 nm respectively, demonstrated significant antiplasmodial activity against the Plasmodium parasites, and over the extracts of *Moringa oleifera* stem bark and roots. These results express the potential of the green-synthesized IONPs as effective antimalarial agents. Therefore, it is recommended to synthesize iron nanoparticles from isolated active antiplasmodial compounds from *Moringa oleifera* and other medicinal plants to enhance their therapeutic efficacy. However, further work on toxicity and clinical trials are required on the synthesized nanomaterials. In addition, conducting comprehensive histopathological analyses to assess the toxicity of IONPs in major organs is crucial for ensuring their safety for clinical use. Similar work on other pathogens could further show the versatility and potential of IONPs in treating various infectious diseases

References

[1] WHO. 2023. **World malaria Report. 2023**. Vol. WHO/HTM/GM, *World Health Organization*.. 1–283 .

[2] Wassmer SC, Taylor TE, Rathod PK, Mishra SK, Mohanty S, Arevalo-Herrera M, Manoj T. Duraisingh, and Joseph D. Smith. 2015. **Investigating the pathogenesis of severe malaria: A multidisciplinary and cross-geographical approach.** *American Journal of Tropical Medicine and Hygiene* 2015;93(Suppl 3):42–56.

[3] Albohiri HH, and Alzanbagi NA. 2021. **Systemic Review on the Pathogenicity of Plasmodium berghei in the Liver and Spleen of the Experimental Mice.** Journal of Pharmaceutical Research International (July):515–29.

[4] Breman JG. 2009. **Eradicating malaria.** *Sci Prog.* 92(1):1–38.

[5] Bekono BD, Ntie-Kang F, Onguéné PA, Lifongo LL, Sippl W, Fester K, and Owono Luc C. O. 2020. **The potential of anti-malarial compounds derived from African medicinal plants: A review of pharmacological evaluations from 2013 to 2019.** *Malaria Journal.* 19(1):1–35.

[6] Negm WA, Ezzat SM, and Zayed A. 2023. **Marine organisms as potential sources of natural products for the prevention and treatment of malaria.** *RSC Advances* 13(7):4436–75.

[7] Waluyo D, Prabandari EE, Pramisandi A, Hidayati DN, Chrisnayanti E, Puspitasari DJ, et al. 2021 **Exploring natural microbial resources for the discovery of anti-malarial compounds.** *Parasitology International* 85:102432.

[8] Tiwari VS, Joshi P, Yadav K, Sharma A, Chowdhury S, Manhas A,, Kumar N., Tripathi R., and Haq W., 2021. **Synthesis and Antimalarial Activity of 4-Methylaminoquinoline Compounds against Drug-Resistant Parasite.** *ACS Omega.* 6(20):12984–94.

[9] Neves Borgheti-Cardoso L, San Anselmo M, Lantero E, Lancelot A, Serrano JL, Hernández-Ainsa S, Fernàndez-Busquets X, and Sierra, T. 2020. **Promising nanomaterials in the fight against malaria.** *Journal of Materials Chemistry B.* 8(41):9428–48.

[10] Bhatt V, Kumari S, Upadhyay P, Agrawal P, Anmol, Sahal D, Sharma U. 2020. **Chemical profiling and quantification of potential active constituents responsible for the antiplasmodial activity of Cissampelos pareira.** *Journal of Ethnopharmacol*.ogy, 262(December 2019):113185.

[11] Greve HL, Kaiser M, Kaiser M, and Schmidt TJ. 2020. **Investigation of Antiplasmodial Effects of Terpenoid Compounds Isolated from Myrrh.** *Planta Medica* 86(9):643–54.

[12] Dawurung CJ, Nguyen MTH, Pengon J, Dokladda K, Bunyong R, Rattanajak R, Kamchonwongpaisan S, Nguyen PTM and Pyne SG. 2021. **Isolation of bioactive compounds from medicinal plants used in traditional medicine: Rautandiol B, a potential lead compound against Plasmodium falciparum.** *BMC Complementary and Medicine Therapies.* 21(1):1–12.

[13] Osei E, Kwain S, Mawuli GT, Anang AK, Owusu KBA, Camas M, Ohashi M, Alexandru-Crivac C., Deng H, Jaspars M. and Kyeremeh K. 2019. **Paenidigyamycin A, potent antiparasitic imidazole alkaloid from the ghanaian Paenibacillus sp. De2Sh.** *Marine Drugs.* 17(1):1–13.

[14] Smyrniotopoulos V, Merten C, Kaiser M, and Tasdemir D. 2017. **Bifurcatriol, a new antiprotozoal acyclic diterpene from the brown alga Bifurcaria bifurcata.** *Marine Drugs.* 15(8):1–10.

[15] Ju E, Latif A, Kong CS, Seo Y, Lee YJ, Dalal SR, Dalal SR, Casseraa MB and Kingston DGI. 2018. **Antimalarial activity of the isolates from the marine sponge Hyrtios erectus against the chloroquine-resistant Dd2 strain of Plasmodium falciparum.** *Zeitschrift fur Naturforschung - Section C Journal of Biosciences* 73(9–10):397–400.

[16] Qin GF, Tang XL, Sun YT, Luo XC, Zhang J, Van Ofwegen L, Sung, PJ, Li, PL, Li, GQ. 2018. **Terpenoids from the soft coral Sinularia sp. Collected in Yongxing Island.** *Marine Drugs.* 16(4):1–15.

[17] Fontinha D, and Moules I, 2020. Prudêncio M. **Repurposing drugs to fight hepatic malaria**

parasites. Molecules. 25(15).

[18] Pongratz P, Kurth F, Ngoma GM, Basra A, Ramharter M. 2011. **In vitro activity of antifungal drugs against Plasmodium falciparum field isolates.** *Wien Klin Wochenschr.* 123(SUPPL. 1):26–30.

[19] Setyaningrum E, Arifiyanto A, Nukmal N, Aeny TN, Putri M handerlin, Setiawati UN mah. 2021. **In vitro test for inhibition of plasmodium falciparum 3d7 parasites using streptomyces hygroscopicus subsp. hygroscopicus strain i18, isolated from a Pineapple Farm in lampung.** *J Pure Appl Microbiol.* 15(2):891–6.

[20] Niu G, Hao Y, Wang X, Gao JM, Li J. 2020. **Fungal metabolite asperaculane b inhibits malaria infection and transmission.** *Molecules*. 25(13):1–13.

[21] Fröhlich T, Reiter C, Ibrahim MM, Beutel J, Hutterer C, Zeitträger I, et al. 2017 **Synthesis of Novel Hybrids of Quinazoline and Artemisinin with High Activities against Plasmodium falciparum, Human Cytomegalovirus, and Leukemia Cells.** *ACS Omega.* 2(6):2422–31.

[22] Silva AF, Torres MDT, Silva LS, Alves FL, Miranda A, Oliveira VX, et al. 2024. **Synthetic angiotensin II peptide derivatives confer protection against cerebral and severe non-cerebral malaria in murine models.** *Sci Rep*. 14(1):1–9.

[23] Sivakumar R, Floyd K, Jessey E, Kim JK, Bayguinov PO, Fitzpatrick JAJ, et al. 2024. **Poly-basic peptides and polymers as new drug candidate against Plasmodium falciparum**. *Malaria Journal.* 23: 227

[24] Tsamesidis I, Lymperaki E, Egwu CO, Pouroutzidou GK, Kazeli K, Reybier K, Bourgeade-Delmas S, Valentin A and Kontonasaki E. 2021. **Effect of silica based nanoparticles against plasmodium falciparum and leishmania infantum parasites.** *Journal of Xenobiotics.* 11(4):155–62.

[25] Kumar S, Shukla MK, Sharma AK, Jayaprakash GK, Tonk RK, Chellappan DK, et al. 2023. **Metal-based nanomaterials and nanocomposites as promising frontier in cancer chemotherapy.** *MedComm.* 4(2):1–26.

[26] El-Barkey NM, Nassar MY, El-Khawaga AH, Kamel AS, Baz MM. 2023. **Efficacy of alumina nanoparticles as a controllable tool for mortality and biochemical parameters of Culex pipiens.** *Scientific Report.* 13(1):1–13.

[27] Torkashvand H, Dehdast SA, Nateghpour M, Haghi AM, Fard GC, Elmi T, Shabani M, Fatemeh and Tabatabaie F. 2023. **Antimalarial nano-drug delivery system based on graphene quantum dot on Plasmodium falciparum: Preparation, characterization, toxicological evaluation.** *Diamond and Related Materials.* 132(December 2022):109670.

[28] Samimi S, Maghsoudnia N, Eftekhari RB, Dorkoosh F. 2018. **Lipid-Based Nanoparticles for Drug Delivery Systems [Internet]. Characterization and Biology of Nanomaterials for Drug Delivery: Nanoscience and Nanotechnology in Drug Delivery.** *Elsevier Inc.* 47–76.

[29] Kekani LN, Witika BA. 2023. **Current advances in nanodrug delivery systems for malaria prevention and treatment**. *Discover Nano.* Vol. 18(1).

[30] Stevens DM, Crist RM, Stern ST. 2021. **Nanomedicine Reformulation of Chloroquine and Hydroxychloroquine.** *Molecules.* 26(1) 175.

[31] Andrade RGD, Veloso SRS, Castanheira EMS. 2020. **Shape anisotropic iron oxide-based magnetic nanoparticles: Synthesis and biomedical applications.** *International Journal of Molecular Science* 21(7) 2455.

[32] Attia NF, El-Monaem EMA, El-Aqapa HG, Elashery SEA, Eltaweil AS, El Kady M, Khalifa SMA, Hawash HB, El-Seedi HR. 2022. **Iron oxide nanoparticles and their pharmaceutical applications.** *Applied Surface Science Advances* 11(April):100284.

[33] Besenhard MO, LaGrow AP, Hodzic A, Kriechbaum M, Panariello L, Bais G, et al. 2020. **Co-precipitation synthesis of stable iron oxide nanoparticles with NaOH: New insights and continuous production via flow chemistry.** *Chemical Engineering Journal*. 399(January):125740.

[34] Yang H, Wang H, Wen C, Bai S, Wei P, Xu B, et al. 2022. **Effects of iron oxide nanoparticles as T 2-MRI contrast agents on reproductive system in male mice.** *Journal of Nanobiotechnology.* 20(1):1–18.

[35] Turrina C, Berensmeier S, Schwaminger SP. 2021. **Bare iron oxide nanoparticles as drug delivery carrier for the short cationic peptide lasioglossin.** *Pharmaceuticals*. 14(5).

[36] Mu Q, Lin G, Jeon M, Wang H, Chang FC, Revia RA, Yu J,and Zhanget M. 2021. **Iron oxide nanoparticle targeted chemo-immunotherapy for triple negative breast cancer.** *Material Today.* 50(November):149–69.

[37] Vassallo M, Martella D, Barrera G, Celegato F, Coïsson M, Ferrero R, et al. 2022. **Improvement of Hyperthermia Properties of Iron Oxide Nanoparticles by Surface Coating.** *ACS Omega.* 2023; 2143-2154.

[38] Chen C, Meng Q, Liu Z, Liu S, Tong W, An B, Ding B, Ma P., Ling J. 2023. **Iron oxide-EDTA nanoparticles for chelation-enhanced chemodynamic therapy and ion interference therapy.** *Biomaterial Sciences.* 11(13):4549–56.

[39] Arias LS, Pessan JP, Vieira APM, De Lima TMT, Delbem ACB, Monteiro DR. 2018. **Iron oxide nanoparticles for biomedical applications: A perspective on synthesis, drugs, antimicrobial activity, and toxicity.** *Antibiotics*. 7(46) 1-32.

[40] Ba-Abbad MM, Benamour A, Ewis D, Mohammad AW, and Mahmoudi E. 2022. **Synthesis of Fe_3O_4 Nanoparticles with Different Shapes Through a Co-Precipitation Method and Their Application.**

Journal of the Minerals. 74(9):3531–9.

[41] Lassenberger A, Grünewald TA, Van Oostrum PDJ, Rennhofer H, Amenitsch H, Zirbs R, Lichtenegger HC and Reimhult E. 2017. **Monodisperse Iron Oxide Nanoparticles by Thermal Decomposition: Elucidating Particle Formation by Second-Resolved in Situ Small-Angle X-ray Scattering.** *Chemistry Materials.* 29(10):4511–22.

[42] Liu T, Zhang S, and Xu Y. 2022. **Preparation and characterization of Fe_3O_4 nanoparticles via a hydrothermal process with propanediol as the solvent.** *Material Research Express.* 9(12), 125001.

[43] Ni X, Zhang J, Zhao L, Wang F, He H, Dramou P. 2022. **Study of the solvothermal method time variation effects on magnetic iron oxide nanoparticles (Fe_3O_4) features.** *Journal of Physics and Chemistry of Solids.* 169, 110855.

[44] Asab G, Zereffa EA, Abdo Seghne T. 2020. **Synthesis of Silica-Coated Fe_3O_4 Nanoparticles by Microemulsion Method: Characterization and Evaluation of Antimicrobial Activity.** *International Journal of Biomaterials.* 2020, 1-11.

[45] Tahir H, Saad M, Latif M, Tanweer Hyder S, Ahmed R. 2024. **Synthesis of Metal Oxide Nano Particles by Sol-Gel Method and Investigation of its Biomedical Applications.** *Nanochemistry Research.* 9(1):19–27.

[46] Qu J, Cheah P, Adams D, Collen C, and Zhao Y. 2024. **The influence of the polyol solvents on the continuous growth of water-dispersible iron oxide nanoparticles.** *Journal of Material Research*. 39(1):165–75.

[47] Braim FS, Razak Nnana, Aziz AA, Dheyab MA, and Ismael LQ. 2023. **Optimization of ultrasonic-assisted approach for synthesizing a highly stable biocompatible bismuth-coated iron oxide nanoparticles using a face-centered central composite design**. *Ultrasonic Sonochemi*stry 95(March):106371.

[48] Sequeira CAC. 2018. **Electrochemical Synthesis of Iron Oxide Nanoparticles for Biomedical Application.** *Organic and Medicinal Chemistry International Journal.* 5(2), 555660.

[49] Muthukumar B, Duraimurugan R, Parthipan P, Rajamohan R, Rajagopal R, Narenkumar J, Rajasekar A and Malik T 2024. **Synthesis and characterization of iron oxide nanoparticles from Lawsonia inermis and its effect on the biodegradation of crude oil hydrocarbon.** *Scientific Report.* 14:11335–45.

[50] Daramola OB, George RC, Torimiro N, and Olajide AA. 2024. **Insights on the synthesis of iron-oxide nanoparticles and the detection of iron-reducing genes from soil microbes.** *Colloids Surfaces C: Environmental Aspects.* 2:100025.

[51] Shabbir MA, Naveed M, Rehman S ur, Ain N ul, Aziz T, Alharbi M, et al. 2023. **Synthesis of Iron Oxide Nanoparticles from Madhuca indica Plant Extract and Assessment of Their Cytotoxic, Antioxidant, Anti-Inflammatory, and Anti-Diabetic Properties via Different Nanoinformatics Approaches.** *ACS Omega.* 2023;8(37):33358–66.

[52] Mirza AU, Kareem A, Nami SAA, Khan MS, Rehman S, Bhat SA, et al. 2018. **Biogenic synthesis of iron oxide nanoparticles using Agrewia optiva and Prunus persica phyto species: Characterization, antibacterial and antioxidant activity.** *Journal of Photochemistry and Photobiology B: Biology.* 185:262–74.

[53] Yassin MT, Al-Otibi FO, Al-Askar AA, Alharbi RI. 2023. **Green Synthesis, Characterization, and Antifungal Efficiency of Biogenic Iron Oxide Nanoparticles.** *Applied Science* 13(17).

[54] Alamu GA, Ayanlola PS, Babalola KK, Adedokun O, Sanusi YK, Fajinmi GR. 2024. **Green synthesis and characterizations of magnetic iron oxide nanoparticles using Moringa oleifera extract for improved performance in dye-sensitized solar cell.** *Chemical Physics Impact.* 8(December 2023):100542.

[55] Perumalsamy H, Balusamy SR, Sukweenadhi J, Nag S, MubarakAli D, El-Agamy Farh M., Vijay H and Rahimi S. 2024. **A comprehensive review on Moringa oleifera nanoparticles: importance of polyphenols in nanoparticle synthesis, nanoparticle efficacy and their applications.** *Journal of Nanobiotechnology*. 22(1):1–27.

[56] Yesmin S, Mahiuddin M, Nazmul Islam ABM, Karim KMR, Saha P, Khan MAR., Ahsan HM. 2024. **Piper chaba Stem Extract Facilitated the Synthesis of Iron Oxide Nanoparticles as an Adsorbent to Remove Congo Red Dye.** *ACS Omega.* 9(9):10727–37.

[57] Kobylinska N, Klymchuk D, Shakhovsky A, Khainakova O, Ratushnyak Y, Duplij V, et al. 2021. **Biosynthesis of magnetite and cobalt ferrite nanoparticles using extracts of "hairy" roots: preparation, characterization, estimation for environmental remediation and biological application.** RSC Advances.11(43): 26974–87.

[58] Mangundayao K, and Yasurin P. 2017. **Bioactivity of Moringa oleifera and its Applications: A Review.** *Journal of Pure and Applied Microbiology* 11(1):43–50.

[59] Attah AF, Moody JO, Sonibare MA, Salahdeen HH, Akindele OO, Nnamani PO, Diyaolu OA, and Raji Y. 2020. **Aqueous extract of Moringa oleifera leaf used in Nigerian ethnomedicine alters conception and some pregnancy outcomes in Wistar rat.** *South African Journal of Botany*. 129:255–62.

[60] Elemike EE, Joe P, Ikenweke C, Onwudiwe D, Omotade ET, and Singh M. 2023. **Synthesis , characterization , anti-cancer and antimicrobial studies of iron oxide nanoparticles mediated by Terminalia catappa (Indian almond) leaf extract.** *Inorganic Chemistry Communication.* 155(March):111048.

[61] Gitau W, Edinah, Kwamboka Songoro Jeremiah, Waweru Gathirwa Francis K, Kariuki HN. 2023. I**n vivo**

antiplasmodial activities of stem bark extracts of Avicennia marina in Plasmodium berghei - infected mice. *Pan African Medical Journal* 44(93):1–19.

[62] Ishaya YL, Mankilik MM, Idoko ED. 2019. **Anti-plasmodial Activity of Chloroform Leaf Extract of Eucalyptus camaldulensis in Mice.** *African Journal of Biomedical Research* 22:303–7.

[63] Okokon JE, Mobley R, Edem UA, Bassey AI, Fadayomi I, Drijfhout F, Horrocks P, and Li W. 2022. **In vitro and in vivo antimalarial activity and chemical profiling of sugarcane leaves.** *Scientific Reports* 12(1):1–13.

[64] Shahid H, Shah AA, Shah Bukhari SNU, Naqvi AZ, Arooj I, Javeed M, et al. 2023. **Synthesis, Characterization, and Biological Properties of Iron Oxide Nanoparticles Synthesized from Apis mellifera Honey.** *Molecules*, 28(18): 2504.

[65] Tawfik EK, Eisa WH, Okasha N, and Ashry HA. 2020. **Influence of annealing temperature of α-Fe_2O_3 nanoparticles on Structure and Optical Properties.** *Journal of Scientific Research in Science.* 37(1):1–20.

[66] Viju Kumar VG, Prem AA. 2018. **Green synthesis and characterization of iron oxide nanoparticles using phyllanthus niruri extract.** *Oriental Journal of Chemistry.* 34(5):2583–9.

[67] Hwang SW, Umar A, Dar GN, Kim SH, and Badran RI. 2014. **Synthesis and characterization of iron oxide nanoparticles for phenyl hydrazine sensor applications.** *Sensor Letters.* 12(1):97–101.

[68] Kgosiemang IKR, Adegoke AM, Mashele SS, and Sekhoacha MP. 2023. **Green synthesis of Iron oxide and Iron dioxide nanoparticles using Euphorbia tirucalli: characterization and antiproliferative evaluation against three breast cancer cell lines.** *Journal of Experimental Nanoscience* 18(1) 2276276.

[69] Jegadeesan GB, Srimathi K, Santosh Srinivas N, Manishkanna S, Vignesh D. 2019. **Green synthesis of iron oxide nanoparticles using Terminalia bellirica and Moringa oleifera fruit and leaf extracts: Antioxidant, antibacterial and thermoacoustic properties.** *Biocatalysis and Agricultural Biotechnoly*. 21(August):101354.

[70] Ndou N, Rakgotho T, Nkuna M, Doumbia IZ, Mulaudzi T, and Ajayi RF. 2023. **Green Synthesis of Iron Oxide (Hematite) Nanoparticles and Their Influence on Sorghum bicolor Growth under Drought Stress.** *Plants.* 12(7):1–23.

[71] Lunin A V., Sokolov IL, Zelepukin I V., Zubarev I V., Yakovtseva MN, Mochalova EN, et al. 2020. **Spindle-like MRI-active europium-doped iron oxide nanoparticles with shape-induced cytotoxicity from simple and facile ferrihydrite crystallization procedure.** *RSC Advances.* 10(12):7301–12.

[72] Kiwumulo HF, Muwonge H, Ibingira C, Lubwama M, Kirabira JB, Ssekitoleko RT. 2022. **Green synthesis and characterization of iron-oxide nanoparticles using Moringa oleifera: a potential protocol for use in low and middle income countries.** *BMC Research Notes.* 15(1):1–8.

[73] Jamzad M, Kamari Bidkorpeh M. 2020. **Green synthesis of iron oxide nanoparticles by the aqueous extract of Laurus nobilis L. leaves and evaluation of the antimicrobial activity.** *Journal of Nanostructure in Chemistry.* 10(3):193–201.

[74] Dehbi A, Dehmani Y, Omari H, Lammini A, Elazhari K, Abdallaoui A. 2020. **Hematite iron oxide nanoparticles (α-Fe_2O_3): Synthesis and modelling adsorption of malachite green.** *Journal of Environmental Chemical Engineering* 8(1):103394.

[75] Malik V, Pal A, Pravaz O, Crassous JJ, Granville S, Grobety B, et al. 2017. **Hybrid magnetic iron oxide nanoparticles with tunable field-directed self-assembly.** *Nanoscale.* 9(38):14405–13.

[76] Selvaraj SP. 2022. **Enhanced surface morphology of copper oxide (CuO) nanoparticles and its antibacterial activities.** *Materials Today: Proceedings* 50(7): 2865–8.

[77] Bin M, Hossain S, Chowdhury F, Ahmed S. 2022. **Synthesis and characterization of CuO nanoparticles utilizing waste fish scale and exploitation of XRD peak profile analysis for approximating the structural parameters.** *Arabian Journal of Chemistry* 15(10):104117.

[78] Muhaimin M, Chaerunisaa AY, Rostinawati T, Amalia E, Hazrina A, Nurhasanah S. 2023. **A Review on Nanoparticles of Moringa Oleifera Extract: Preparation, Characterization, and Activity.** *International Journal of Applied Pharmaceutics.* 15(4):43–51.

[79] Nadeem F, Fozia F, Aslam M, Ahmad I, Ahmad S, Ullah R, et al. 2022. **Characterization, Antiplasmodial and Cytotoxic Activities of Green Synthesized Iron Oxide Nanoparticles Using Nephrolepis exaltata Aqueous Extract.** *Molecules.* 27:4931.

[80] Kannan D, Yadav N, Ahmad S, Namdev P, Bhattacharjee S, Lochab B, et al. 2019. **Pre-clinical study of iron oxide nanoparticles fortified artesunate for efficient targeting of malarial parasite.** *EBioMedicine*. 45:261–77.

[81] Lazcano-Ramírez HG, Garza-García JJO, Hernández-Díaz JA, León-Morales JM, Macías-Sandoval AS, García-Morales S. 2023. **Antifungal Activity of Selenium Nanoparticles Obtained by Plant-Mediated Synthesis.** *Antibiotics.*12(1); 115.

Cite this article

Fayomi O.M., Olajide O.O. and Emmanuel S.A. (2025). Anti-Plasmodial Activity of Iron Oxide Nanoparticles Derived from *Moringa Oleifera* Stem Bark and Root Extracts. FUAM Journal of Pure and Applied Science, **5**(**1**):10-22